Adsorption of dissolved organic matter on clay minerals as assessed by infra-red, CPMAS 13C NMR spectroscopy and low field T1 NMR relaxometry.

Adsorption of dissolved organic matter on clay minerals as assessed by infra-red, CPMAS ^{13}C NMR spectroscopy and low field T1 NMR relaxometry

Pellegrino Conte[a], Cristina Abbate[b], Andrea Baglieri[b], Michele Negre[c],Claudio De Pasquale[a], Giuseppe Alonzo [a], Mara Gennari [b]

[a] Dipartimento dei Sistemi Agro-Ambientali, Università degli Studi di Palermo, v.le delle Scienze, edificio 4, 90128 Palermo, Italy
[b] Dipartimento di Scienze Agronomiche, Agrochimiche e delle Produzioni Animali, Universita‘ di Catania, via S. Sofia 98, 95123 Catania, Italy
[c] Dipartimento di Valorizzazione e Protezione delle Risorse Agroforestali, Università degli Studi di Torino, via Leonardo da Vinci 44, 10095 Grugliasco (To), Italy

ABSTRACT

Dissolved organic matter (DOM) is a very important environmental constituent due to its role in controlling factors for soil formation, mineral weathering and pollutant transport in the environment. Prediction of DOM physical–chemical properties is achieved by studying its chemical structure and spatial conformation. In the present study, dissolved organic matter extracted from compost obtained from the organic fraction of urban wastes (DOM-P) has been analysed by FT-IR, CPMAS 13C NMR spectroscopy and 1H T1 NMR relaxometry with fast field cycling (FFC) setup. While the first two spectroscopic techniques revealed the chemical changes of dissolved organic matter after adsorption either on kaolinite (DOMK) or montmorillonite (DOM-S), the latter permitted the evaluation of the conformational variations as assessed by longitudinal relaxation time (T1) distribution at the fixed magnetic field of 500 mT. Alterations of T1 distributions from DOM-P to DOM-K and DOM-S were attributed to a decreasing molecular complexity following DOM-P adsorption on the clay minerals. This study applied for the first time solid state 1H T1 NMR relaxometry to dissolved organic matter from compost obtained from the organic fraction of urban wastes and revealed that this technique is very promising for studying environmentally relevant natural organic systems.

1. Introduction

Dissolved organic matter (DOM) originates from plant litter, soil humus, microbial biomass and root exudates (Kalbitz et al., 2000). As for soil organic matter, a general chemical definition of DOM is impossible, but it is often operationally reported as a continuum of organic molecules with different sizes and structures that pass through a filter of 0.45 lm pore size (Herbert and Bertsch, 1995; Kalbitz et al., 2000). However, many studies used different filter sizes making the quantitative comparison among experimental results very complicated (Herbert and Bertsch, 1995). Notwithstanding the difficulties in finding an objective DOM definition, it must be emphasized that it is very important in the regulation of hypolimnetic metabolism of large lakes (Kim et al., 2006), in promotion of phytoplankton blooms (Boyer et al., 2006) and as a major controlling factor in soil formation (Petersen 1976; Dawson et al., 1978; Uselman et al., 2007), mineral weathering (Lindroos et al., 2003), and pollutant transport (Kalbitz et al., 1997; Temminghoff et al., 1997; Marschner, 1999; Persson et al., 2003; Blasioli et al., 2008; Barrioso et al., 2010). In addition, interactions of dissolved organic matter with soil mineral components strongly influence soil carbon cycle (Kaiser, 1998; Hansell and Carlson, 2001; Gaberell et al., 2003; Kahle et al., 2003; Cookson and Murphy, 2004; Ravichandran, 2004; Park, 2009). For this reason, DOM characterization and analysis of DOM interactions with clay minerals have a relevant importance for the understanding of its role in ecosystem functioning.

Typical analytical approaches for DOM characterization are fluorescence and absorbance spectroscopy (Chefetz et al., 1998; Baker and Spencer, 2004; Rivero et al., 2004; Velasco et al., 2004; Koch et al., 2008; Park, 2009), cross polarization magic angle spinning (CPMAS) 13C NMR spectroscopy (Kaiser et al., 2003; Conte et al., 2004), and high resolution liquid state 1H NMR spectroscopy (Lam and Simpson, 2008). Recently, Fourier transform ion cyclotron mass spectrometry (FT-ICR-MS) has been applied to evaluate physico-chemical DOM characteristics as related to molecular formulas (Koch et al., 2008). To the best of our knowledge, low field 1H T1 NMR relaxometry with fast field cycling (FFC) has never been applied to the identification of DOM conformational properties. The technique is based on the cycling of the Zeeman magnetic field (B0) through three different values traditionally indicated as polarization (Bpol), relaxation (Brelax) and acquisition (Bacq) fields (Kimmich and Anoardo, 2004; Ferrante and Sykora, 2005). Bpol is applied for a limited and ixed period of time in order to obtain magnetization saturation and sensitivity enhancement (Kimmich and Anoardo, 2004). Then, the magnetic field is switched to a new one, Brelax, applied for a period (s) during which the intensity of the magnetization changes (or relaxes) to reach a new equilibrium condition. Finally, the application of the acquisition magnetic field together with a 1H 90_ pulse makes the magnetization observable and the free induction decay (FID) acquirable. The proton longitudinal relaxation times are obtained
at the fixed Brelax intensity through a progressive variation of the s values. Longitudinal relaxation time (T1) represents the lifetime of the first order rate process that returns the 1H magnetization to the Boltzman equilibrium along the z axis (Bakhmutov, 2004). The T1 magnitude depends on the nature of the nuclei, the physical state of the system and the temperature. In particular, spin–lattice relaxation occurs when the lattice experiences magnetic fields fluctuating at frequencies resembling those of the observed nuclei (e.g. protons). Fluctuating fields are obtained by molecular motions which strongly affect dipolar interactions (Bakhtumov, 2004). Namely, the faster the motions (e.g., in small sized molecular systems), the lower is the dipolar interaction efficiency, thereby favouring longer T1 values (Bakhtumov, 2004). Conversely, slower molecular dynamics (as in large sized molecules) can be associated with shorter spin–lattice relaxation times due stronger nuclear dipolar interactions (Bakhtumov, 2004). In the present study, dissolved organic matter has been extracted from the compost obtained from the organic fraction of urban wastes. After adsorption on clay minerals (montmorillonite and kaolinite), FT-IR and CPMAS 13C NMR spectroscopy were applied to recognize DOM structural changes. The spectroscopic results were used to support DOM conformational changes as revealed by solid state low field 1H T1 NMR relaxometry with fast field cycling (FFC) setup at a Brelax of 500 mT.

2. Materials and methods

2.1. Preparation of dissolved organic matter

Dissolved organic matter was prepared according to the procedure of Gigliotti et al. (1997). Briefly, 100 g of the compost obtained from the organic fraction of urban wastes were added to 1 l of deionised and degassed water and shaken overnight at room temperature.
After centrifugation (20 min at 2795 g), the supernatant was separated and filtered first through a 0.7 lm GF/C glass filter (Whatman Corp. Springfield Mill, UK) and then through a 0.45 lm Supor-450 polysulfone membrane (Pall Gelman Sciences,
Ann Arbor, MI, USA). The liquid was finally freeze dried and the solid material (DOM-P) used for the spectroscopic analyses.

2.2. DOM adsorption on clays

A montmorillonite (Wyoming smectite SWy-2, Crook County, Wyoming, USA) and a kaolinite (Washington County, Georgia, USA) were purchased from Source Clay Mineral Depository (Colombia, MO, USA) and used without further purification. Ten grams of each clay were suspended in 110 ml of a 5.0 mg/ml DOM solution. After 24 h shaking at room temperature, the mixtures containing either kaolinite or montmorillonite were centrifuged at 15,000 g for 30 min and then filtered through a 0.45 lm Supor-450 polysulfone membrane (Pall Gelman Sciences, Ann Arbor, MI, USA). The supernatants obtained after interaction with kaolinite (DOM-K) and montmorillonite (DOM-S) were freeze dried and used for the solid state spectroscopic analyses.

2.3. FT-IR spectroscopy

Infra-red spectroscopy analyses were conducted with a Nicolet 6700 FT-IR spectrometer (Thermo-scientific, MA, USA) with a resolution of 4 cm_1 within a wavenumber range of 4000–400 cm_1. Eight scans were used to acquire each spectrum by using OMNIC
7.3 software. All the samples were analysed in the solid state after preparation of pellets. The pellets were prepared by finely grinding 2 mg of each freeze dried DOM (-P, -K or -S) in an agate mortar, together with 98 mg of R-grade KBr (Sigma, Milano, Italy). All the DOM-KBr mixtures were ground in a ball mill before being compressed into pellets.

2.4. CPMAS ^{13}C NMR

Cross polarization magic angle spinning 13C NMR (CPMAS 13C NMR) spectra were acquired by using a Bruker Avance-II 400 spectrometer (Bruker Biospin, Milan, Italy) operating at 100.6 MHz on 13C and equipped with a 4 mm standard bore solid state probe.
Samples were packed into a 4 mm zirconia rotor with Kel-F cap and the rotor spin rate was set at 13,000 ± 1 Hz. In total, 4 k data points (TD) were collected over an acquisition time (AQ) of 50 ms, a recycle delay (RD) of 2.0 s, and 1024 scans (NS). Contact time (CT) was 1 ms. All spectra were acquired with a 1H RF field of 40 kHz and a ramp of 7 kHz. The radio frequency field applied
to 13C during the spin lock pulse was set at 51 kHz. The 1H RAMP sequence was used to account for possible inhomogeneities of the Hartmann–Hahn matching condition at high rotor spin rates (Conte et al., 2004). The recycle delay was chosen after evaluation
of T1(H) values in order to fix RD > 5T1(H) (Conte et al. 2004). Contact time was set at 1 ms after evaluation of variable contact time experiments as described in Conte et al. (1997). Precise 1H 90_ pulse calibration for CP acquisition was obtained as reported in Conte and Piccolo (2007). Bruker Topspin_ 2.0 software was used to acquire all the spectra. Spectra elaboration was conducted by Mestre-C software (Version 4.9.9.9, Mestrelab Research, Santiago de Compostela, Spain). Free induction decays (FID) were transformed by applying first a 4 k zero filling and then an exponential filter function with a line broadening (LB) of 100 Hz. Fully automatic baseline correction using a Bernstein algorithm was applied for baseline correction (Brown, 1995).

2.5. Solid state low field 1H T1 NMR relaxometry

A Stelar Spinmaster-FFC-2000 field-cycling relaxometer (Stelar s.r.l., Mede, PV – Italy) was used to run T1 NMR relaxometry experiments. The solid state DOM samples were studied at the constant probe temperature of 298 K. The experimental relaxometry setting consisted of a polarization field with a flux density of 580 mT corresponding to a proton Larmor frequency (xL) of 25 MHz applied for a period of time (Tpol) of 0.1 s; a relaxation field with a flux density of 500 mT (xL = 20 MHz) chosen inside the highest sensitivity
instrumental region and applied for a period s arrayed with 64 values varying from 1 to 800 ms. The s array was chosen in a geometrical progression in order to cover the entire relaxation curve of interest. Finally, a 380 mT (xL = 16.2 MHz) acquisition field with a 1H 90_ pulse of 7 ls was

applied in order to obtain observable magnetization and reveal free induction decay (FID) with a time domain of 100 ls sampled with 512 points. 512 scans were accumulated. Acquisition of relaxation curves was achieved with the AcquNMR V95_ software provided by Stelar. The experimental data were processed with UPEN algorithm (Alma Mater Studorium, Universita di Bologna), which gives the distributions of T1 values (Borgia et al., 1998, 2000). The T1 distribution curves (also indicated as relaxograms) were exported to OriginPro 7.5 SR6 ((Version 7.5885, OriginLab Corporation, Northampton, MA, USA) in order to perform deconvolution with Gaussian functions and to recover the different components giving rise to the longitudinal relaxation time distributions. The number of Gaussian functions that were used for the deconvolution without unreasonably increasing the number of parameters were determined by means of the Merit function analysis (Halle et al., 1998).

3. Results and discussion

3.1. FT-IR analyses

Fig. 1A shows the FT-IR spectrum of the dissolved organic matter used in the present study before adsorption on clays (DOM-P).
The spectrum is typical for DOM systems (Kaiser et al., 1997; Kovac et al., 2002; Vane et al., 2008) and a detailed spectral assignment is reported in Table 1. After interactions with kaolinite, the resulting DOM-K sample revealed a spectrum (Fig. 1B) with few modifications: (1) the bands due to the stretching vibrations of CH_2 and CH_3 groups (2963, 2926 and 2850 cm_1) and those assigned to the C–O stretching vibrations in carbohydrates and alcohols (between 1000 and 1100 cm^{-1}) show larger intensity compared to Fig. 1A; (2) the intensity of the band associated to the aromatic ring stretching vibrations, to the C–H in-plane deformations and possibly to COO^- stretching vibrations (1402 cm^{-1}) is lower than that reported in the spectrum of DOM-P (Fig. 1B). These results can be explained by the ability of kaolinite to adsorb aromatic systems.
In fact, Harris et al. (2001) and Zhang et al. (2009) reported that kaolinite can be used to remove polycyclic aromatic hydrocarbons and azobenzenes from aqueous solutions through formation of Van der Waals interactions between clay surface and the planar structures of the aromatic rings. As a consequence, all the FT-IR bands which are hidden under the aromatic signal in DOM-P spectrum (Fig. 1A) become more accentuated and intense in the spectrum of DOM-K (Fig. 1B).
As DOM-P adsorbs on montmorillonite, DOM-S sample is retrieved.
Comparison between DOM-P (Fig. 1A), DOM-K (Fig. 1B) and DOM-S (Fig. 1C) spectra revealed that an intensity decrease of the band at 1651 cm^{-1}, disappearing of the signal at 1402 cm_1 and decrease of the bands between 1100 and 900 cm^{-1} occurred in the spectrum of DOM-S. These results appear in line with the findings from Sutton et al. (2005). In fact, these authors showed that montmorillonite interacts with –OH containing systems through formation of H-bonds via two different mechanisms. On the one hand, –OH containing molecules move closer to clay surface being attracted by the surficial oxygen in montmorillonite. The –OH groups in alcohol-like molecules and in acid systems act as proton donors for the formation of surficial H bridges with the clay system. On the other hand, clay surface cavities, due to a lack of nearby charge compensating inter-layer cations, may attract the small water molecules present in DOM solutions. Water, in turn, can form H-bonds with the hydrophilic DOM moieties, thereby acting as a bridge between the organic systems and the clay mineral. As the supernatant in equilibrium with the solid clay phase is removed, oxydril-containing organic molecules remain adsorbed and a FT-IR spectrum of DOM-S (Fig. 1C) with less intense C–O stretching vibration bands as compared to the spectra of DOM-P (Fig. 1A) and DOM-K (Fig. 1B) resulted.

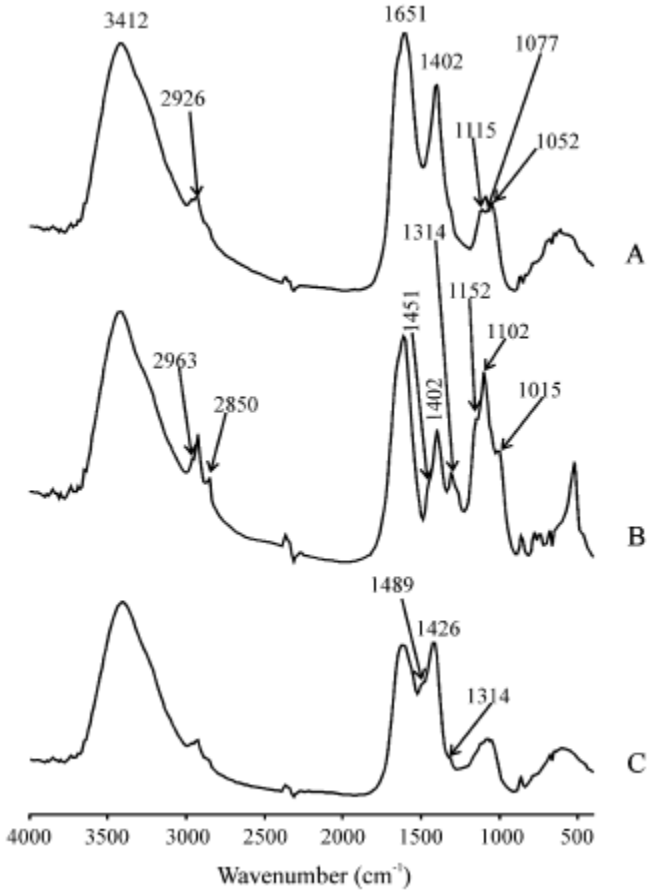

Fig. 1. FT-IR spectra of dissolved organic matter (DOM-P, A) and the dissolved organic matter after interaction with kaolinite (DOM-K, B) and montmorillonite (DOM-S, C).

Table 1
FT-IR spectral assignment of dissolved organic matter (DOM) used in the present study.

Wavenumber, cm^{-1}	Spectral assignment
3412	Hydrogen bonded –OH and –NH groups
2963, 2926, 2850	Symmetric and asymmetric stretching vibrations of primarily CH_2 and CH_3 groups
1651	C=O stretching of amide I
1402	Aromatic rings stretching vibrations; C–H in-plane deformations; COO– stretching vibrations
1100–900	C–O stretching of carbohydrates and alcohols

3.2. CPMAS 13C NMR spectra

The CPMAS 13C NMR spectrum of the dissolved organic matter before interactions with clay minerals (DOM-P) is reported in Fig. 2A. Figs. 2B and C report the spectra of DOM after

interaction with kaolinite (DOM-K) and montmorillonite (DOM-S), respectively. All the spectra reveal the typical NMR signal pattern of humic-like materials (Wilson, 1987). In fact, as expected, six different intervals are recognized (Wilson, 1987; Conte et al., 2004). The first one, between 0 and 45 ppm, is attributed to alkyl systems. The most important signals in this interval are a shoulder at 18 ppm and two large bands at 24 and 30 ppm. In addition, a signal at 39 ppm is present only in the spectra of DOM-K (Fig. 2B) and DOM-S (Fig. 2C). The resonance at 18 ppm is usually assigned to methyl groups (Wilson, 1987), while the bands at 24 and 30 ppm are attributed to linear methylene (–CH2–) chains (Wilson, 1987; Roscoe et al., 2004) belonging either to cutin-like structures or to other aliphatic rich bio-moieties (Nierop et al., 2001). The signal at 39 ppm (spectra of DOM-K and DOM-S) is due to the resonance of secondary methyne carbons (–CH–) possibly generated by chlorophyll-like and terpene-like systems (Skjemstad et al., 1983).
The second spectral interval between 45 and 60 ppm is traditionally attributed to nitrogenated and oxygenated alkyl systems (Wilson, 1987; Conte et al., 2004). However, the sole signal visible in all the spectra is at 56 ppm conceivably due to oxygenated carbons. In fact, according to Wilson (1987), only O-alkyl groups such as methoxyls in lignin-like structures or –CH2O– systems into branched molecules can resonate at that chemical shift value.

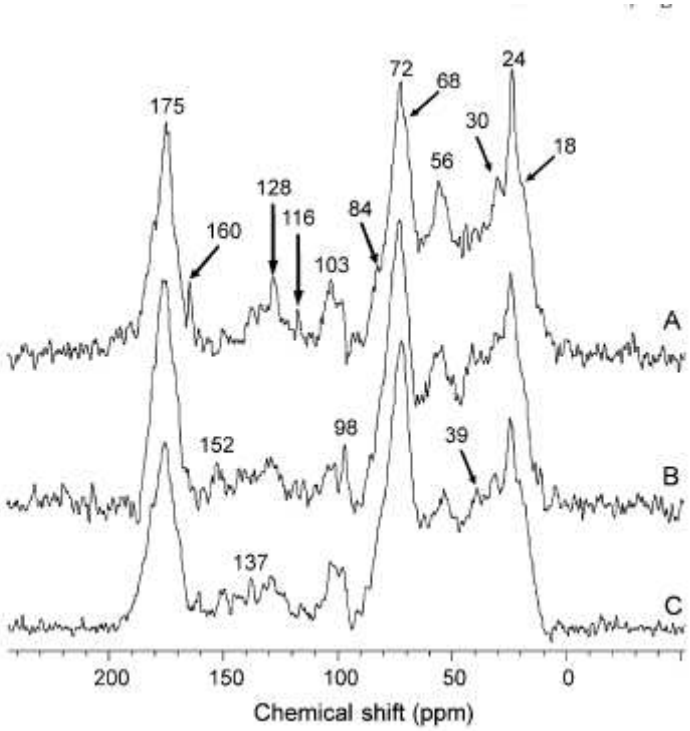

Fig. 2. CPMAS 13C NMR spectra of dissolved organic matter (DOM-P, A), and the dissolved organic matter after interaction with kaolinite (DOM-K, B) and montmorillonite (DOM-S, C).

The region in the chemical shift interval 60–90 ppm is indicative of the presence of carbohydrates with the largest contribution due to celluloses and hemicelluloses (Schmidt et al., 2000; Lemma et al., 2007; Taylor et al., 2008). In particular, the shoulders at 68 and 84 ppm can be due to carbon 6 and 4 respectively, while the signal at 72 ppm is usually assigned to carbons in positions 2, 3 and 5 in cellobiose units. Signals of carbohydrates are also observed in the range 90–120 ppm. Here the resonance at 103 ppm can be attributed to C1 of cellobiose units into cellulose I, while that at

around 98 ppm is assigned to the acetal carbons in the xylane systems inside hemicelluloses (Larsson et al., 1999; Schmidt et al., 2000). The 90–120 ppm interval also contains a signal at 116 ppm which is attributable to acetal carbons in cellulose II-like systems.
The spectral region that is usually assigned to aromatic moieties is 120–160 ppm. In particular, the spectrum of DOM-P (Fig. 2A) reveals a main signal centered at 128 ppm, whereas DOM-K and DOM-S (Figs. 2B and C, respectively) show also signals at 137 and _152 ppm. All these signals are assigned to lignin systems (Roscoe et al., 2004). In particular, p-hydroxyphenol derivative structures are assumed to give a signal at around 128 ppm, O-aryl carbons from guaiacyl-like and syringil-like units may give resonances at 137 and 152 ppm. Finally, the last spectral region between 160 and 190 ppm is attributable to –COOH groups. The visual inspection of Fig. 2 reveals that the relative intensity of the signal at 24 ppm is larger in DOM-P than in DOM-K and DOM-S spectra. Moreover, the latter two spectra also show appearance of signals at 39, 137 and 152 ppm with the contemporary intensity diminution of the resonance at 128 ppm. Finally, DOMS spectrum uncovers intensity reduction of the signals at 56 and 175 ppm. All these findings confirm FT-IR results. In fact, as part of DOM-P is retained on kaolinite and montmorillonite (such as lignin-like structures), a reduction of signal intensity in the alkyl (0–45 ppm) and aromatic (120–160 ppm) regions arises. Proportionally, sensitivity enhancement for the signals attributable to chlorophyll-like, terpene-like, guaiacyl-like and syringil-like systems is achieved. The recorded changes are similar in both DOM-K and DOM-S CPMAS 13C NMR spectra, thereby revealing that both clays can adsorb hydrophobic systems in accordance with literature data (Harris et al., 2001; Sutton et al., 2005; Zhang et al., 2009). In addition, however, the signal intensity decrease at 56 and 175 ppm in the spectrum of DOM-S (Fig. 2C) indicates that montmorillonite also adsorbs hydrophilic compounds as already reported in literature (Sutton et al., 2005) and in the FT-IR section of the present study.

3.3. Longitudinal relaxation time distributions

Fig. 3A reports the relaxogram of DOM-P. It shows a complex T1 distribution which was deconvoluted in five different relaxing components centered at 3, 6, 19, 55 and 121 ms. The number of relaxing components certainly accounts for the DOM-P molecular complexity which was already described in many papers (Chefetz et al., 1998; Gigliotti et al., 1997; Koch et al., 2008; Vane et al., 2008) and in the spectroscopic analyses reported here.

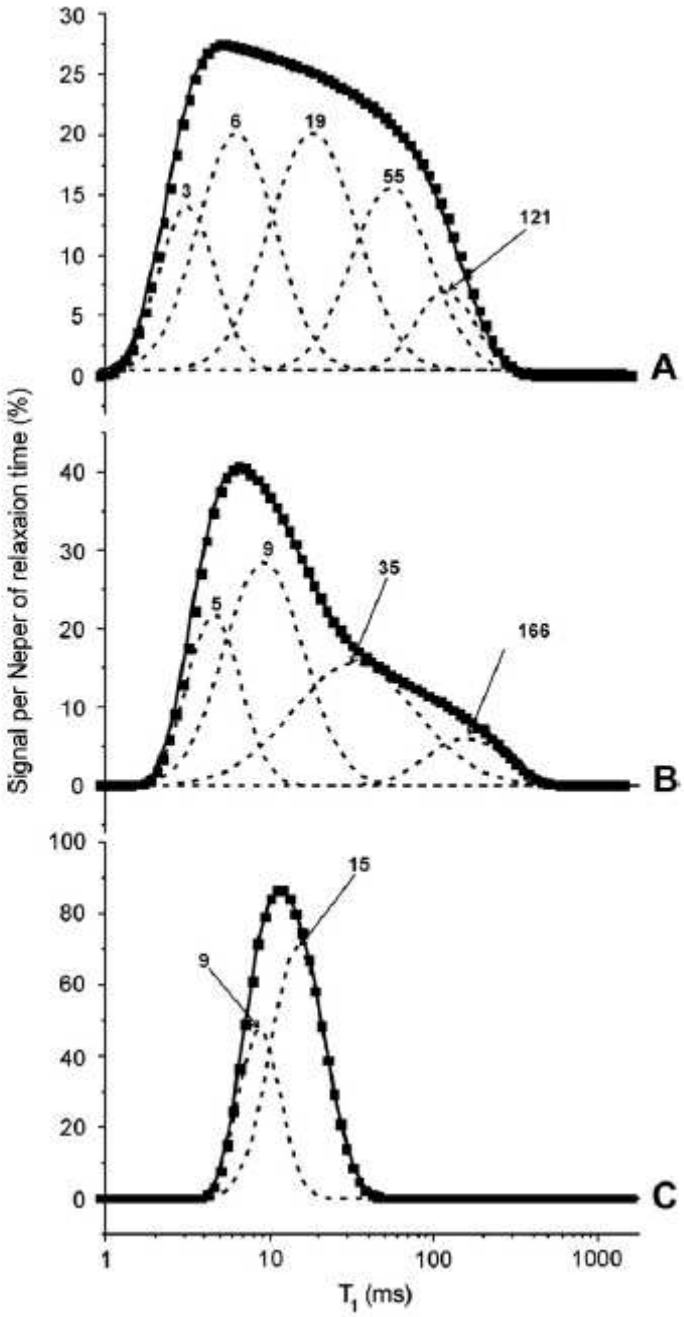

Fig. 3. 500 mT relaxograms of dissolved organic matter (DOM-P, A), and dissolved organic matter after interaction with kaolinite (DOM-K, B) and montmorillonite (DOM-S, C). The black dots are the experimental data. The dashed lines represent the different T1 components as obtained by deconvolution. The full lines are the fitting of the experimental data obtained by deconvolution.

DOM-P can be considered as a complex mixture of different organic molecules among which hydrophobic alkyl and aromatic systems and hydrophilic peptidic and saccharidic moieties play the major roles (Gigliotti et al., 1997). These components form supramolecular associations held together by dispersive forces (e.g. p– p, CH–p, and Van der Waals forces), thereby promoting formation of aggregates with a wide distribution of molecular sizes (Conte and Piccolo, 1999). After freeze drying, the smaller sized DOM-P solid aggregates are subjected to fast rotational

motions which lead longitudinal relaxation time towards longer values (increasing T1 values in Fig. 3A). Conversely, the slow rotational motions affecting larger DOM-P aggregates promote more efficient intraand inter-proton dipolar interactions. For this reason, shorter longitudinal relaxation time values are obtained (decreasing T1 values in Fig. 3A). As dissolved organic matter interacts with kaolinite, adsorption on a clay surface and conformational re-arrangement of the organic matter occurs. Adsorption of organic moieties was indicated by FT-IR and CPMAS 13C NMR spectroscopy (see above). On the other hand, the DOM-K relaxogram in Fig. 3B reveals that the deconvoluted T1 distribution is made by four components all centered at T1 values (i.e. 5, 9, 35 and 166 ms) different from those found for DOM-P sample. Following interaction with kaolinite, all the organic DOM-K components occurring in the supernatant solution reaggregate, thereby promoting a new distribution of aggregate sizes and a new apportionment of the T1 values (Fig. 3B). The relaxogram of DOM-S appears significantly simpler than that of DOM-K as only two T1 components at 9 and 15 ms were apparent after deconvolution (Fig. 3C). A conceivable explanation for this experimental evidence can be related to the different layer structure of montmorillonite which can adsorb small organic matter components not only on its surface, but also in its inter-layers. As a consequence, the amount of organic matter retrieved after interaction with montmorillonite is lower than that recovered after interaction with kaolinite.

4. Conclusions

This study presented a chemical-physical characterization of dissolved organic matter extracted from compost obtained from the organic fraction of urban wastes before and after adsorption on two clay minerals (i.e. kaolinite and montmorillonite). FT-IR and CPMAS 13C NMR spectroscopy indicated that kaolinite adsorbed preferentially hydrophobic DOM components, whereas montmorillonite showed higher affinity for hydrophilic –OH containing moieties. Following adsorption on clay minerals, a conformational re-arrangement of the DOM subunits was observed by application of 1H T1 NMR relaxometry with a fast field cycling setup. This latter technique revealed that a simplification of the relaxograms occurred when DOM-P was adsorbed either on kaolinite (DOM-K) or on montmorillonite (DOM-S). In particular, the number of relaxometric components varied in the order DOMP > DOM-K > DOM-S. According to literature data (Chefetz et al., 1998; Gigliotti et al., 2002; Koch et al., 2008; Vane et al., 2008) and to the FT-IR and CPMAS 13C NMR spectroscopy results, the higher relaxometric complexity of DOM-P reflected its molecular complexness. In fact, dissolved organic matter is a mixture of molecules resulting from the degradation of plant materials, humus, biomasses and root exudates. All of them associate in superstructures having a wide distribution of different molecular sizes (Conte and Piccolo, 1999), thereby producing the distribution of T1 values reported in Fig. 3A. After adsorption on kaolinite and montmorillonite, the remaining organic moieties of the dissolved organic matter re-aggregate to form new superstructures with a different T1 distribution as compared to DOM-P. Finally, the simplest T1 distribution of DOM-S was explained by considering the inter-layer adsorption capacity of montmorillonite which enabled the retention of a larger amount of organic molecules than kaolinite. Although the combination with conventional spectroscopy (i.e. FT-IR and CPMAS 13C NMR) provided a good basis for the comprehension of DOM relaxograms, much more must still be done to retrieve additional and more detailed relaxometric information. In fact, field cycling NMR relaxometry can be used to investigate the underlying correlation functions (Kimmich and Anoardo, 2004; Ferrante and Sykora, 2005; Conte et al., 2009a,b; Pohlmeier et al., 2009; Pru˚šova et al., 2010) which in turn contain the physical information needed for the understanding of the nature of the interactions involved in the complexation of natural organic matter (such as DOM) and the organic and inorganic components of the environmental compartments.

Acknowledgment

This work was partially funded by Ce.R.T.A. s.c.r.l. (Centri Regionali per le Tecnologie Alimentari; http://www.certa.it/default. asp). The authors are grateful to Centro Grandi Apparecchiature – UniNetLab of Universita degli Studi di Palermo (http://www. unipa.it/cga/index.html) for having provided machine time at the high field NMR spectrometer.

References

Baker, A., Spencer, R.G.M., 2004. Characterization of dissolved organic matter from source to sea using fluorescence and absorbance spectroscopy. Science of the Total Environment 333, 217–232.
Bakhmutov, V.L., 2004. Pratical NMR Relaxation for Chemists. John Wiley & Sons Ltd., Chichester, West Sussex, UK. Barrioso, E., Andrades, M.-S., Benoit, P., Houot, S., 2010. Pesticide desorption from soils facilitated by dissolved organic matter coming from compost: experimental data and modelling approach. Biogeochemistry on-line First. doi: 10.1007/s10533-010-9481-y.
Blasioli, S., Braschi, I., Pinna, M.V., Pusino, A., Gessa, C.A., 2008. Effect of undesalted dissolved organic matter from composts on persistence, adsorption, and mobility of cyhalofop herbicide in soils. Journal of Agricultural and Food Chemistry 56, 4102–4111.
Borgia, G.C., Brown, R.J.S., Fantazzini, P., 1998. Uniform-penalty inversion of multiexponential decay data. Journal of Magnetic Resonance 132, 65–77.
Borgia, G.C., Brown, R.J.S., Fantazzini, P., 2000. Uniform-penalty inversion of multiexponential decay data II: data spacing, T2 data, systematic data errors, and diagnostics. Journal of Magnetic Resonance 147, 273–285.
Boyer, J.N., Dailey, S.K., Gibson, P.J., Rogers, M.T., Mir-Gonzalez, D., 2006. The role of dissolved organic matter bioavailability in promoting phytoplankton blooms in Florida Bay. Hydrobiologia 569, 71–85.
Brown, D.E., 1995. Fully automated baseline correction of 1D and 2D NMR spectra using Bernstein algorithm. Journal of Magnetic Resonance A 114, 268–270.
Chefetz, B., Adani, F., Genevini, P., Tambone, F., Hadar, Y., Chen, Y., 1998. Characterization of dissolved organic matter extracted from composted municipal solid waste. Soil Science Society of American Journal 62, 326–332.
Conte, P., Piccolo, A., 1999. Conformational arrangement of dissolved humic substances. Influence of solution composition on association of humic molecules. Environmental Science and Technology 33, 1682–1690.
Conte, P., Piccolo, A., van Lagen, B., Buurman, P., de Jager, P.A., 1997. Quantitative aspects of solid-state 13C-NMR spectra of humic substances from volcanic soils. Geoderma 80, 327–338.
Conte, P., Spaccini, R., Piccolo, A., 2004. State of the art of CPMAS ^{13}C-NMR spectroscopy applied to natural organic matter. Progress in Nuclear Magnetic Resonance Spectroscopy 44 (3–4), 215–223.
Conte, P., Piccolo, A., 2007. Precise measurement of 1H 90_ pulse in solid-state NMR spectroscopy for complex and heterogeneous molecular systems. Analytical and Bioanalytical Chemistry 387, 2903–2909.
Conte, P., Maccotta, A., De Pasquale, C., Bubici, S., Alonzo, G., 2009a. Dissolution mechanism of crystalline cellulose in H3PO4 as assessed by high-field NMR spectroscopy and fast field cycling NMR relaxometry. Journal of Agricultural and Food Chemistry 57, 8748–8752.
Conte, P., Bubici, S., Palazzolo, E., Alonzo, G., 2009b. Solid state 1H-NMR relaxation properties of the fruit of a wild relative of eggplant at different proton Larmor frequencies. Spectroscopy Letters 42, 235–239.
Cookson, W.R., Murphy, D.V., 2004. Quantifying the contribution of dissolved organic matter to soil nitrogen cycling using 15N isotopic pool dilution. Soil Biology and Biochemistry 36, 2097–2100.
Dawson, H.J., Ugolini, F.C., Hrutfiord, B.F., Zachara, J., 1978. Role of soluble organics in the soil processes of a podzol, Central Cascades, Washington. Soil Science

126, 290–296.
Ferrante, G., Sykora, S., 2005. Technical aspects of fast field cycling. Advances in Inorganic Chemistry 57, 405–470.
Gaberell, M., Chin, Y.-P., Hug, S.J., Sulzberger, B., 2003. Role of dissolved organic matter composition on the photoreduction of Cr(VI) to Cr(III) in the presence of iron. Environmental Science and Technology 37, 4403–4409.
Gigliotti, G., Giusquiani, P.L., Businelli, D., Macchioni, A., 1997. Composition changes of dissolved organic matter in a soil amended with municipal waste compost. Soil Science 162, 919–926.
Halle, B., Johannesson, H., Venu, K., 1998. Model-free analysis of stretched relaxation dispersions. Journal of Magnetic Resonance 135, 1–13.
Hansell, D.A., Carlson, C.A., 2001. Marine dissolved organic matter and the carbon cycle. Oceanography 14, 41–49.
Harris, R.G., Wells, J.D., Johnson, B.B., 2001. Selective adsorption of dyes and other organic molecules to kaolinite and oxide surfaces. Colloids and Surfaces 180, 131–140.
Herbert, B.E., Bertsch, P.M., 1995. Characterization of dissolved and colloidal organic matter in soil solution: a review. In: Kelly, J.M., McFee, W.W. (Eds.), Carbon forms and functions in forest soils. SSSA, Madison, WI, pp. 63–88.
Kaiser, K., Guggenberger, G., Haumaier, L., Zech, W., 1997. Dissolved organic matter sorption on subsoils and minerals studied by 13C-NMR and DRIFT spectroscopy. European Journal of Soil Science 48, 301–310.
Kaiser, K., 1998. Fractionation of dissolved organic matter affected by polyvalent metal cations. Organic Geochemistry 28, 849–854.
Kaiser, E., Simpson, A.J., Dria, K.J., Sulzberger, B., Hatcher, P.G., 2003. Solid-state and multidimensional solution-state NMR of solid phase extracted and ultrafiltered riverine dissolved organic matter. Environmental Science and Technology 37, 2929–2935.
Kahle, M., Kleber, M., Jahn, R., 2003. Retention of dissolved organic matter by illitic soils and clay fractions: influence of mineral phase properties. Journal of Plant Nutrition and Soil Science 166, 737–741.
Kalbitz, K., Solinger, S., Park, J.-H., Michalzik, B., Matzner, E., 2000. Controls on the dynamics of dissolved organic matter in soils: a review. Soil Science 165 (4), 277–304.
Kalbitz, K., Popp, P., Geyer, W., Hanschmann, G., 1997. D-HCH mobilization in polluted wetland soils as influenced by dissolved organic matter. Science of the Total Environment 204, 37–48.
Kim, C., Nishimura, Y., Nagata, T., 2006. Role of dissolved organic matter in hypolimnetic mineralization of carbon and nitrogen in a large, monomictic lake. Limnology and Oceanography 51 (1), 70–78.
Kimmich, R., Anoardo, E., 2004. Field-cycling NMR relaxometry. Progress in Nuclear Magnetic Resonance Spectroscopy 44, 257–320.
Koch, B.P., Ludwichowski, K.-U., Kattner, G., Dittmar, T., Witt, M., 2008. Advanced characterization of marine dissolved organic matter by combining reversephase liquid chromatography and FT-ICR-MS. Marine Chemistry 111, 233–241.
Kovac, N., Bajt, O., Faganelli, J., Sket, B., Orel, B., 2002. Study of macroaggregate composition using FT-IR and 1H-NMR spectroscopy. Marine Chemistry 78, 205–215.
Lam, B., Simpson, A.J., 2008. Direct 1H NMR spectroscopy of dissolved organic matter in natural waters. Analyst 133, 263–269.
Larsson, P.T., Hult, E.-L., Wickholm, K., Pettersson, E., Iversen, T., 1999. CPMAS ^{13}CNMR spectroscopy applied to structure and interaction studies on cellulose I. Solid State Nuclear Magnetic Resonance 15, 31–40.
Lemma, B., Nilsson, I., Kleja, D.B., Olsson, M., Knicker, H., 2007. Decomposition and substrate quality of leaf litters and fine roots from three exotic plantations and a native forest in the southwestern highlands of Ethiopia. Soil Biology and Biochemistry 39, 2317–2328.

Lindroos, A.-J., Brugger, T., Derome, J., Derome, K., 2003. The weathering of mineral soil by natural soil solutions. Water, Air, and Soil Pollution 149, 269–279.
Marschner, B., 1999. Sorption von polyzyklischen aromatischen Kohlenwasserstoffen (PAK) und olychlorierten Biphenylen im Boden. Journal of Plant Nutrition and Soil Science 162, 1–14.
Nierop, K.G.J., van Lagen, B., Buurman, P., 2001. Composition of plant tissues and soil organic matter in the first stages of a vegetation succession. Geoderma 100, 1– 24.
Park, J.-H., 2009. Spectroscopic characterization of dissolved organic matter and its interactions with metals in surface waters using size exclusion chromatography. Chemosphere 77, 485–494.
Persson, L., Alsberg, T., Odham, G., Ledin, A., 2003. Measuring the pollutant transport capacity of dissolved organic matter in complex matrixes. International Journal of Environmental and Analytical Chemistry 83, 971–986.
Petersen, L., 1976. Podzols and Podzolization. DSR Forlag, Kopenhagen.
Pohlmeier, A., Haber-Pohlmeier, S., Stapf, S., 2009. A fast field cycling nuclear magnetic resonance relaxometry study of natural soils. Vadose Zone Journal 8, 735–742.
Prusova, A., Conte, P., Kucerik, J., Alonzo, G., 2010. Dynamics of hyaluronan aqueous solutions as assessed by fast field cycling NMR relaxometry. Analytical and Bioanalytical Chemistry 397, 3023–3028.
Ravichandran, M., 2004. Interactions between mercury and dissolved organic matter a review. Chemosphere 55, 319–331.
Rivero, C., Chirenje, T., Ma, L.Q., Martinez, G., 2004. Influence of compost on soil organic matter quality under tropical conditions. Geoderma 123, 355–361.
Roscoe, R., Buurman, P., Van Lagen, B., 2004. Transformations in occluded light fraction organic matter in a clayey oxisol; evidence from 13C-CPMAS-NMR and d13C signature. Revista Brasileira de Ciencia do Solo 28, 811–818.
Schmidt, M.W.I., Knicker, H., Kogel-Knabner, I., 2000. Organic matter accumulating in Aeh and Bh horizons of a Podzol-chemical characterization in primary organo-mineral associations. Organic Geochemistry 31, 727–734.
Skjemstad, J.O., Frost, R.L., Barron, P.F., 1983. Structural units in humic acids from south-eastern Queensland soils as determined by 13C NMR spectroscopy. Australian Journal of Soil Science 21, 539–547.
Sutton, R., Sposito, G., Diallo, M.S., Schulten, H.-R., 2005. Molecular simulation of a model of dissolved organic matter. Environmental Toxicology and Chemistry 24, 1902–1911.
Taylor, R.E., French, A.D., Gamble, G.R., Himmelsbach, D.S., Stipanovic, R.D., Thibodeaux, D.P., Wakelyn, P.J., Dybowski, C., 2008. 1H and 13C solid-state NMR of Gossypium barbadense (Pima) cotton. Journal of Molecular Structure 878, 177–184.
Temminghoff, E.J.M., Vander-Zee, S.E.A.T.M., de Haan, F.A.M., 1997. Copper mobility in a copper-contaminated sandy soil as affected by pH and solid and dissolved organic matter. Environmental Science and Technology 31, 1109–1115.
Uselman, S.M., Qualls, R.G., Lilienfein, J., 2007. Contribution of root vs. leaf litter to dissolved organic carbon leaching through soil. Soil Science Society of American Journal 71, 1555–1563.
Vane, C.H., Alexander, K., Antoni, M., Smellie, J., West, J., 2008. Molecular characterization of dissolved organic matter (DOM) in ground waters from the Aspo underground research laboratory, Sweden: a novel ‘‘finger printing’’ tool for palaeohydrological assessment. In: Scientific Basis for Nuclear Waste Management, Sheffield, 2007, USA, Materials Research Society, pp. 557–565.
Velasco, M.I., Campitelli, P.A., Ceppi, S.B., Havel, J., 2004. Analysis of humic acid from compost of urban wastes and soil by fluorescence spectroscopy. Agriscientia 21, 31–38.
Wilson, MA., 1987. NMR Techniques and Applications in Geochemistry and Soil Chemistry. Pergamon Press, Oxford, UK.
Zhang, X., Hong, H., Li, Z., Guan, J., Schulz, L., 2009. Removal of azobenzene from water by kaolinite. Journal of Hazardous Materials 170, 1064–1069.